

# Signatures of Mode Conversion and Kinetic Alfvén Waves at the Magnetopause

Jay R. Johnson,<sup>1</sup> C. Z. Cheng,<sup>1</sup> and P. Song<sup>2,3</sup>

**Abstract.** It has been suggested that resonant mode conversion of compressional MHD waves into kinetic Alfvén waves at the magnetopause can explain the abrupt transition in wave polarization from compressional to transverse commonly observed during magnetopause crossings [Johnson and Cheng, 1997b]. We analyze magnetic field data for magnetopause crossings as a function of magnetic shear angle (defined as the angle between the magnetic fields in the magnetosheath and magnetosphere) and compare with the theory of resonant mode conversion. The data suggest that amplification in the transverse magnetic field component at the magnetopause is not significant up to a threshold magnetic shear angle. Above the threshold angle significant amplification results but with weak dependence on magnetic shear angle. Waves with higher frequency are less amplified and have a higher threshold angle. These observations are qualitatively consistent with theoretical results obtained from the kinetic-fluid wave equations.

## Introduction

Ultra-low frequency (ULF) waves (with frequencies below 500 mHz) dominate the spectrum of nearly every magnetopause crossing [Perraut *et al.*, 1979; Rezeau *et al.*, 1993; Song *et al.*, 1993; Song, 1994; Phan and Paschmann, 1996; and references therein]. It has been suggested that these waves are associated with mode conversion of MHD waves in the magnetosheath to kinetic Alfvén waves (KAWs) at the magnetopause near a field line resonance location [Lee *et al.*, 1994; Belmont *et al.*, 1995; De Keyser *et al.*, 1999]. The mode conversion process can explain (a) a change in wave polarization at the magnetopause and (b) the amplification of the transverse magnetic field component by an order of magnitude [Johnson and Cheng, 1997b]. In this work, we present evidence that ULF waves at the magnetopause result from a mode conversion process which transforms compressional MHD waves that originate in the magnetosheath into transverse KAWs. Based on a data survey of ISEE1, ISEE2, and WIND magnetopause crossings, we examine the dependence of the mode conversion process on the magnetic shear angle (defined as the angle between the magnetic field in the magnetosheath and magnetosphere on each side of the magnetopause). The results of the sur-

vey compare favorably with theoretical predictions [Johnson and Cheng, 1997b].

## Magnetosheath/Magnetopause Wave Activity and Magnetic Shear

The most striking wave feature of magnetopause crossings is the sharp transition in the polarization of low frequency wave power from compressional ( $\delta B_{\parallel} \geq \delta B_{\perp}$ ) in the magnetosheath to transverse ( $\delta B_{\perp} \gg \delta B_{\parallel}$ ) at the magnetopause [Rezeau *et al.*, 1993; Song *et al.*, 1993; Song, 1994; Phan and Paschmann, 1996; and references therein]. An example of such a transition is illustrated by the WIND crossing of the magnetopause on December 12, 1996 shown in Fig. 1. During this period WIND was passing from the flank magnetosheath into the magnetosphere ( $X_{gse} \sim 0$ ,  $Y_{gse} \sim 15R_E$ ,  $Z_{gse} \sim 0$ ). Around 19:00 UT the magnetic field vector rotated by  $60^\circ$  due to a rotation of the solar wind magnetic field [Phan *et al.*, 1997] and the density began to drop gradually. The outer edge of the magnetopause current layer is marked by a distinct magnetic field rotation at 19:20 UT. The satellite moved into the low-latitude boundary layer marked by a rapid density drop at about 19:55 UT and into the plasma sheet at 20:45 UT. The Alfvén velocity increased gradually by a factor of 5 during the magnetopause crossing and the magnetic field vector rotated by around  $50^\circ$ . While in the magnetosheath proper (prior to 19:20 UT), the wave power is mainly in the compressional component as evidenced in the large fluctuations of  $B_{tot}$ . The plasma  $\beta$  for this period is moderate (around 2) and the pressure anisotropy is not very large (see Fig. 2 from Phan *et al.*, [1997])—suggestive that the waves are compressional Alfvén waves rather than mirror modes. The compressional wave activity continues through the magnetopause even though the plasma  $\beta$  gradually drops below unity between 19:20 and 19:55 UT. As the density gradually decreases and the magnetic field increases, the transverse component of the magnetic field fluctuations becomes dominant (note the marked increase in wave activity in the individual GSM Cartesian components of the magnetic field while  $B_{tot}$  fluctuations remain roughly the same). The enhanced transverse wave activity persists all the way into the low-latitude boundary layer from (20:00 UT to 20:45 UT). This magnetopause crossing is typical when compressional wave activity is found in the magnetosheath.

The change in wave polarization from the magnetosheath to the magnetosphere is clearly seen in the power spectrogram for the crossing. Power spectra are obtained for all magnetic field components and the magnetic field magnitude and are used to obtain the compressional and transverse magnetic field spectrum. In Fig. 2 we show the wave power spectral density of compressional,  $P_{\parallel}$ , and transverse,  $P_{\perp}$ , magnetic fluctuations as well as the fraction of wave power in the transverse magnetic field component. A broad band

<sup>1</sup>Princeton University, Plasma Physics Laboratory, Princeton, NJ, 08543 (email jrj@pppl.gov, fcheng@pppl.gov)

<sup>2</sup>Space Physics Research Laboratory, University of Michigan, Ann Arbor, MI

<sup>3</sup>Now at University of Massachusetts, Lowell, MA

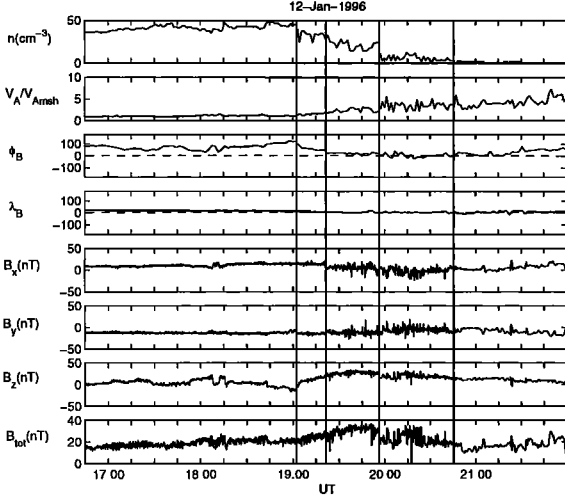


**Figure 1.** Density, Alfvén velocity, and magnetic field data from a magnetopause crossing by the WIND satellite on Jan 12, 1996 from approximately 19:20 UT to 19:55 UT.  $\phi_B$  is the magnetic field vector angle in the LM plane (zero along L axis) and the  $\lambda_B$  is the angle between the magnetic field and the magnetopause tangent plane for a LMN boundary normal coordinate system. Note that in the magnetosheath (prior to 19:20 UT) wave power is primarily compressional. Coincident with the density gradients at the magnetopause is a strong enhancement in the transverse components of the magnetic field fluctuations, but the compressional amplitude remains approximately the same as in the magnetosheath. Data courtesy of R. Lepping and Phan *et al.*, [1997].

of waves is found in the 10–100 mHz frequency range. In the magnetosheath, the waves are primarily compressional, but at the magnetopause, where the density and magnetic field gradients are found, the transverse component is dominant in the same frequency range. The compressional magnetic field spectra remain approximately the same from the magnetosheath into the magnetopause with an eventual cutoff as WIND moved through the low-latitude boundary layer into the plasma sheet at 20:45 UT. In the magnetosheath, the transverse component appears in the same frequency range and is well correlated with the compressional component. However, at the magnetopause there is a dramatic increase in the transverse power spectrum as evidenced in the lower panel of Fig. 2. Note that the amplification (ratio of spectral density at the magnetopause to that of the magnetosheath) of the transverse spectrum falls off as frequency increases.

In order to understand the wave activity better as a function of magnetic shear,  $\theta_{sh}$  (defined as the angle between the magnetic field in the magnetosheath and the magnetic field on the magnetospheric side of the magnetopause), we examined 13 magnetopause crossings using ISEE1, ISEE2, and WIND data. For all crossings, compressional waves were found in the magnetosheath, the spacecraft remained at the magnetopause for an extended time so that spectral analysis could be performed, and the background density gradients were relatively smooth. The wave amplification factor,  $P_{\perp mp}/P_{\perp msh}$ , where  $P_{\perp msh}$  and  $P_{\perp mp}$  refer to average values of the power spectral density of  $\delta\mathbf{B}_{\perp}$  in the magnetosheath and magnetopause respectively, is shown in Fig. 3 for these magnetopause crossings for frequencies of 25 and 50 mHz. The results indicate: (1) the transverse wave component at the magnetopause is not significantly amplified below a threshold angle (approximately  $50^\circ$ ), (2) greatest

amplification is for shear between  $70^\circ$  and  $180^\circ$ , and (3) waves with higher frequencies are less amplified.

## Observations and KAW Theory

These observations can be understood in the context of resonant mode conversion of compressional Alfvén waves into kinetic Alfvén waves (KAW) at the magnetopause. Resonant mode conversion occurs when a compressional Alfvén wave propagates into a region with gradients in  $k_{\parallel}V_A$  such as at the magnetopause where the Alfvén velocity can increase by at least a factor of 10. At the magnetopause, gradients in the direction normal to the magnetopause boundary are dominant compared with gradients along the boundary, and we can approximate the background plasma and magnetic field profiles as functions of the coordinate,  $x$ , in the direction normal to the magnetopause. We assume the magnetic field is of the form  $\mathbf{B} = B_0(x)\mathbf{b}$  where  $\mathbf{b} = \cos\theta_b(x)\hat{z} + \sin\theta_b(x)\hat{y}$  and the magnetic field angle,  $\theta_b$  rotates by an angle  $\theta_{sh}$  across the magnetopause. The equilibrium profiles vary smoothly across the magnetopause on a scale of 10 ion gyroradii ( $\rho_i$ ). For such a configuration, wave propagation is well-described by the kinetic-fluid model [Cheng and Johnson, 1999] which simplifies to the following set of dimensionless coupled equations for  $\mathcal{W}_{\parallel} = \delta p + B_0\delta B_{\parallel}$  and  $\mathcal{W}_x = iB_0\delta B_x$ .

$$\frac{d^2\mathcal{W}_{\parallel}}{dx^2} = -(k_A^2 - k_S^2)\mathcal{W}_{\parallel} + (k_A^2 - k_{\parallel}^2)\delta p + k_{\parallel} \left[ \frac{d}{dx} \log \left( \frac{k_{\parallel}^2}{k_A^2} \right) \right] \mathcal{W}_x \quad (1)$$

$$\begin{aligned} \kappa\mathcal{W}_x &\equiv \left[ 1 + \frac{T_e}{T_i} (1 + \hat{\eta} \frac{Z'_i}{2}) \left( \frac{-2}{Z'_e} \right) \right] k_{\parallel}^2 \rho_i^2 \frac{d^2\mathcal{W}_x}{dx^2} \\ &= (k_{\parallel}^2 - k_A^2) \mathcal{W}_x - k_{\parallel} \frac{d\mathcal{W}_{\parallel}}{dx} \end{aligned} \quad (2)$$

$$\hat{\eta}\mathcal{W}_x \approx \int dx' \frac{dk_x}{2\pi} e^{ik_x(x-x')} b \frac{(\Gamma_0(b) - \Gamma_1(b))}{(1 - \Gamma_0(b))} \mathcal{W}_x(x') \quad (3)$$

$k_S$  is the wavevector in the plane perpendicular to  $x$ ;  $k_{\parallel} = \mathbf{k} \cdot \mathbf{b} = k_S \cdot \mathbf{b} = k_S \cos\theta_{sb}$ , where  $\theta_{sb}$  is the angle between  $\mathbf{b}$  and  $k_S$ ; and  $k_A^2 = \omega^2/V_A^2$  is the Alfvén wavevector where  $\omega$  is the wave frequency and  $V_A$  is the Alfvén velocity.  $Z'_s$  is the derivative of the plasma dispersion function of argument  $\zeta_s = \omega/\sqrt{2}k_{\parallel}v_{ts}$  for species  $s$  with thermal velocity  $v_{ts}$ . We have taken the plasma to be isotropic. The operator  $\hat{\eta}$  is a weakly nonlocal operator introduced by finite Larmor radius effects. The integration involves  $\Gamma_n(b) \equiv I_n(b)e^{-b}$  where  $b \equiv (k_x^2 + k_S^2 \sin^2\theta_b)\rho_i^2$ . Near the location where  $k_{\parallel}^2 = k_A^2$ ,  $\hat{\eta} \approx 1 + \mathcal{O}(\rho_i^2 d^2/dx^2)$  and for  $k_A^2 \gg k_{\parallel}^2$  (as occurs when  $k_{\parallel}$  is small), the contribution of  $\hat{\eta}$  vanishes.

The pressure equation required for the compressional wave is,  $\delta p \approx (1-1/\tau)\mathcal{W}_{\parallel}$  where  $\tau = 1 + \sum_s \beta_s(1+Z'_s/2)$  and summation is over all species,  $s$ . The function  $1/\tau$  is well behaved for the frequencies of interest (in contrast to the MHD approach which gives a singularity where  $\omega^2 = k_{\parallel}^2 C_S^2/(1+\beta)$ ) [De Keyser *et al.*, 1999]. In a cold, isotropic plasma  $\zeta_i \gg 1$ ,  $\tau \rightarrow 1$  and there is no contribution from this term. In a warm plasma with  $\zeta \sim 1$ ,  $\tau \sim \mathcal{O}(1)$  and this term only introduces weak damping to the compressional wave [Johnson and Cheng, 1997a], so the sound resonance is not very important. Moreover, near the Alfvén resonance where  $k_{\parallel}^2 = k_A^2$ , the pressure term vanishes from Eq. 1, and Larmor radius

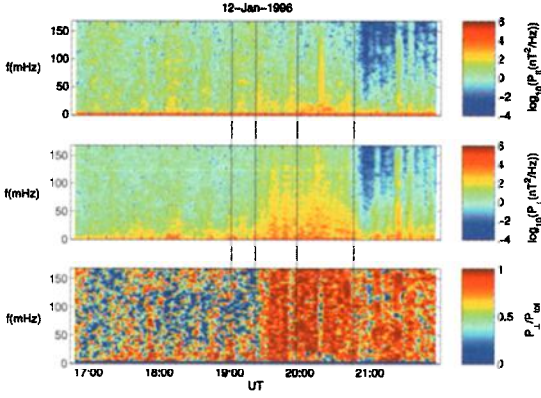


**Figure 2.** Wave power spectra for the WIND crossing of the magnetopause shown in Fig. 1.  $P_{\parallel}$ ,  $P_{\perp}$  and  $P_{tot}$  are the power spectral densities obtained from  $|\delta B_{\parallel}|^2$ ,  $|\delta B_{\perp}|^2$  and  $|\delta \mathbf{B}|^2$  respectively. The change of wave polarization shown in the lower panel coincides with Alfvén velocity gradients encountered upon entry into the magnetopause current layer.

corrections in the term proportional to  $\delta p$  are not critical for describing wave behavior near the Alfvén resonance.

Generally, the Alfvén velocity increases across the magnetopause from the magnetosheath side so that  $k_A^2$  is a monotonically decreasing function. In the magnetosheath the wave is propagating which requires  $k_A^2 > k_S^2$ . As the wave propagates across the magnetopause,  $k_A$  decreases until  $k_A^2 = k_S^2$  where the compressional wave is cutoff. Beyond that location, the compressional wave decays. However, at the location  $k_A^2 = k_{\parallel}^2$  the decaying compressional wave encounters the Alfvén resonance where it can be reflected out of phase from the incoming wave. Near the resonance location the parallel magnetic field is well behaved, but the transverse fields are singular.

Ion gyroradius effects resolve the singular behavior and are described by the kinetic response integral operator,  $\mathcal{K}$  [Cheng and Johnson, 1999]. The model includes the effects of the parallel electric field through the quasineutrality condition, is valid for both large and small  $k_{\perp}^2 \rho_i^2$ , and reduces to the KAW and inertial Alfvén wave dispersion relations in the appropriate limits. (Note that near the location where  $k_{\parallel} \rightarrow 0$ , the wave enters the inertial regime and decays on the scale of the electron skin depth [Cheng and Johnson, 1999]).

We solve Eqs. 1 and 2 numerically on a nonuniform discrete grid and obtain the solutions through matrix manipulation. Boundary conditions are imposed at the magnetosheath and magnetosphere boundaries. The boundary condition in the magnetosheath is an incoming compressional MHD wave. At the magnetosphere boundary, the compressional MHD wave is decaying. For the KAW only radiating/decaying solutions are allowed. Boundary condi-

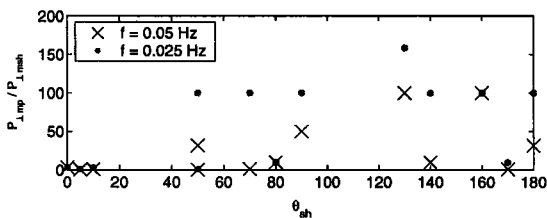


**Figure 3.** Amplification ( $P_{\perp mp}/P_{\perp msh}$ ) of waves at the magnetopause as a function of magnetic shear.

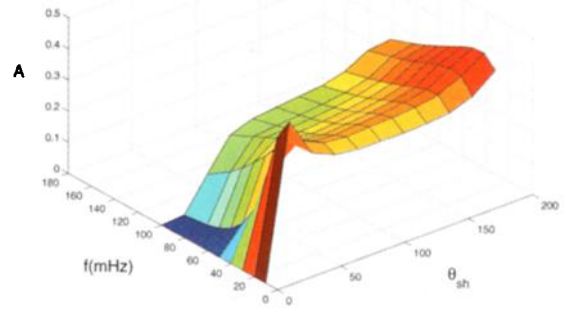


**Figure 4.** Absorption coefficient as a function of frequency and magnetic shear angle  $\theta_{sh}$  (degrees).

tions are imposed asymptotically. The Alfvén velocity is taken to increase by a factor of 10 across the magnetopause and the magnetic field rotates through an angle,  $\theta_{sh}$ .

A good measure of the efficiency of mode conversion at the magnetopause is the amount of compressional wave absorption in the magnetopause layer. Energy absorption is determined by comparing the Poynting flux ( $\delta \mathbf{E} \times \delta \mathbf{B} \cdot \hat{\mathbf{x}}$ ) of the incident compressional wave ( $S_I$ ) with the Poynting flux of the reflected ( $S_R$ ) and transmitted ( $S_T$ ) compressional waves. The Poynting flux of the KAW in the magnetopause near the mode conversion layer is  $S_{KAW} = S_I + S_R - S_T$ . In the magnetopause, the transverse magnetic field component is mainly from the KAW, therefore  $S_{KAW} \sim P_{\perp mp}$ , and the compressional wave absorption,  $A \equiv (S_I + S_R - S_T)/S_I$  is proportional to the wave amplification,  $P_{\perp mp}/P_{\perp msh}$ . Depending on the profiles of  $V_A$  and  $k_S \cdot \mathbf{b}$ , there can be up to three resonance locations in the magnetopause. The absorbed energy is converted to KAWs which: (a) propagate back into the magnetosheath (one resonance location), (b) propagate into both magnetosheath and magnetosphere (two resonance locations), or (c) couple to a quasi-trapped kinetic Alfvén wave (three resonance locations).

To determine the total absorption as a function of frequency and magnetic shear, we sum the absorption over the wavevector spectrum of incoming compressional waves. To do this, we assume that all wavevectors lie on a dispersion surface in wavevector space defined by  $\omega(\mathbf{k}) = \text{const}$  and integrate over the dispersion surface. We integrate over the angles of  $\mathbf{k}$ :  $\theta_{k0}$  is the angle between  $\mathbf{k}$  and the magnetic field in the magnetosheath and  $\phi_{k0}$  is the azimuthal angle in planes perpendicular to the magnetosheath magnetic field,  $\mathbf{B}_{msh}$ . For compressional waves the dispersion surface is approximately defined by  $\omega^2 \approx k^2(V_A^2 + C_s^2 \sin^2 \theta_{k0})$ . The wave vectors are approximately distributed on an ellipsoid with major radius  $k = k_A$  and minor radius  $k = k_A/\sqrt{1 + C_s^2/V_A^2}$ . The absorption spectrum as a function of frequency is obtained by integrating over the ellipsoid—that is, over the angles ( $\theta_{k0}$ ,  $\phi_{k0}$ ) with  $k^2 \approx k_A^2/(1 + C_s^2 \sin^2 \theta_{k0}/V_A^2)$  imposed by the dispersion relation. Moreover, compressional waves typically have  $k_{\perp} \gg k_{\parallel}$  so it is reasonable to assume that the spectrum is highly peaked around  $\theta_{k0} = \pi/2$ . On the other hand, there is no compelling reason to expect that the initial wave spectrum depends on the direction  $\phi_{k0}$ .

The wave observations show a strong dependence of amplification ( $P_{\perp mp}/P_{\perp msh}$ ) on the shear angle across the mag-

netopause. For small shear angles, there is little wave amplification, while above a threshold amplification is enhanced and relatively level. The minimum in amplification for small shear is consistent with the mode conversion mechanism because the waves in the magnetosheath propagate nearly perpendicular to the magnetic field. The absorption coefficient,  $A(\omega, \theta_{sh})$  is presented in Figure 4. The absorption is obtained by computing the absorption coefficient as a function of  $(\omega, \theta_{sh}, \theta_{k0}, \phi_{k0})$  and performing an integration over the variables  $(\theta_{k0}, \phi_{k0})$  with uniform weight in  $\phi_{k0}$  and a strongly peaked weighting function about  $\theta_{k0} = \pi/2$ .

The absorption is the result of mode conversion to KAWs and measures the efficiency of the mode conversion mechanism. The absorbed energy is the Poynting flux of the KAW which radiates away from the mode conversion location. The Poynting fluxes scale as the group velocity multiplied by spectral density. Because the KAW radiates slowly across the magnetic field, its amplitude must be greatly increased compared with the amplitude of the incoming MHD wave in order to carry away the mode converted energy from the field line resonance location. For KAWs the Poynting flux is approximately,  $S_{KAW} \sim (\omega/k_x)k_x^2\rho^2/(1+k_x^2\rho^2)P_{\perp}$ , while for the MHD wave  $S_{MHD} \sim V_A P_{\perp}$ . The KAW wavevector,  $k_x$  can be estimated from dominant balance in Eq. 2— $k_x \sim (\rho_i^2 L)^{-1/3}$  where  $L$  is the scale length of the Alfvén velocity gradient at the magnetopause. One can then estimate from the linear dispersion relation that the wave amplification  $P_{\perp KAW}/P_{\perp MHD} \sim A(1+(\rho/L)^{2/3})V_A/[2\pi f\rho(\rho/L)^{1/3}]$ . For typical magnetopause parameters:  $V_A \sim 300$  km/s,  $\rho_i \sim 50$  km,  $L \sim 500$  km,  $f = 25$  mHz,  $P_{\perp KAW}/P_{\perp MHD} \sim 100A$ .

Because  $|\delta B_{\perp}^2|$  amplification scales directly with compressional wave absorption, the results of Figure 4 can be compared qualitatively with observed  $|\delta B_{\perp}^2|$  amplification. The important features to notice are: (1) for angles greater than  $50^\circ$  the absorption is approximately constant, but for smaller shear there is a trough in  $A$  and (2) the absorption decreases weakly as frequency increases for angles larger than  $50^\circ$ . However, for angles less than  $50^\circ$  there is a significant broadening of the trough for higher frequency with far less absorption. These qualitative properties correspond well to observations of  $|\delta B_{\perp}^2|$  amplification as a function of magnetic shear angle and frequency as discussed in Fig. 3. The quantitative differences between the theory and data (for example, the theoretical threshold angle is smaller) can be attributed to the uncertainly involved in analyzing the data and the simplifications of the theoretical model.

## Discussion and Summary

We examined the dependence of amplification of the transverse magnetic field component at the magnetopause as a function of magnetic shear angle across the magnetopause. The observational events suggest that transverse wave amplification at the magnetopause is not significant up to a threshold angle around 50 degrees. Above this angle significant amplification results. Waves with higher frequencies have less amplification of the transverse magnetic field component and exhibit a wider trough below the threshold. While there was significant amplification of the transverse magnetic power spectra, there was little enhancement of the compressional spectra.

We compared these observations with a theoretical calculation of compressional wave absorption via mode conversion into KAWs at the magnetopause which has been proposed to

be responsible for amplification of the transverse magnetic power spectra. We examined wave absorption as a function of frequency and magnetic shear angle. We integrated over the wavevector spectrum assuming that the incoming wave spectrum is strongly peaked with wavevector perpendicular to the magnetic field in the magnetosheath. The resulting absorption curve suggests that maximum absorption occurs at magnetic shear angles greater than approximately 50 degrees. For smaller angles, a trough in wave absorption is found which is broader for larger frequency. The wave absorption is a decreasing function of frequency for frequencies of interest. These properties are qualitatively consistent with the wave observations. Finally, the mode conversion process does not amplify the compressional magnetic field component consistent with observation.

These results imply that mode conversion of compressional MHD waves to KAWs occurs at the magnetopause. Moreover, based on previous studies the KAWs are expected to provide significant particle transport and plasma heating at the magnetopause [Hasegawa and Mima, 1978; Johnson and Cheng, 1997b].

**Acknowledgments.** This work is supported by NSF grant ATM-9523331 and ATM-9729775.

## References

- Belmont, G., F. Reberac, and L. Rezeau, Resonant amplification of magnetosheath MHD fluctuations at the magnetopause, *Geophys. Res. Lett.*, **22**, 295, 1995.
- Cheng, C. Z., and J. R. Johnson, A kinetic-fluid model, *J. Geophys. Res.*, **104**, 413, 1999.
- De Keyser, J., M. Roth, F. Reberac, L. Rezeau, and G. Belmont, Resonant amplification of MHD waves in realistic subsolar magnetopause configurations, *J. Geophys. Res.*, **104**, 2399, 1999.
- Hasegawa, A., and K. Mima, Anomalous transport produced by kinetic Alfvén wave turbulence, *J. Geophys. Res.*, **83**, 1117, 1978.
- Johnson, J. R., and C. Z. Cheng, Global structure of mirror modes in the magnetosheath, *J. Geophys. Res.*, **102**, 7179, 1997a.
- Johnson, J. R., and C. Z. Cheng, Kinetic Alfvén waves and plasma transport at the magnetopause, *Geophys. Res. Lett.*, **24**, 1423, 1997b.
- Lee, L. C., J. R. Johnson, and Z. W. Ma, Kinetic Alfvén waves as a source of plasma transport at the dayside magnetopause, *J. Geophys. Res.*, **99**, 17405, 1994.
- Perraut, S., R. Gendrin, P. Robert, and A. Roux, Magnetic pulsations observed onboard GEOS 2 in the ULF range during multiple magnetopause crossings, in *Eur. Space Agency Spec. Publ.*, **148**, pp. 113–122, 1979.
- Phan, T. D., and G. Paschmann, Low-latitude dayside magnetopause and boundary layer for high magnetic shear 1. structure and motion, *J. Geophys. Res.*, **101**, 7801, 1996.
- Phan, T. D., et al., Low-latitude dusk flank magnetosheath, magnetopause, and boundary layer for low magnetic shear: Wind observations, *J. Geophys. Res.*, **102**, 19883, 1997.
- Rezeau, L., A. Roux, and C. T. Russell, Characterization of small-scale structures at the magnetopause from ISEE measurements, *J. Geophys. Res.*, **98**, 179, 1993.
- Song, P., Observations of waves at the dayside magnetopause, in *Solar Wind Source of Magnetospheric Ultra-Low-Frequency Waves*, *Geophysical Monograph Series*, vol. 81, pp. 159–171, 1994.
- Song, P., C. T. Russell, R. J. Strangeway, J. R. Wygant, C. A. Cattell, R. J. Fitzenreiter, and R. R. Anderson, Wave properties near the subsolar magnetopause: Pc 3–4 energy coupling for northward interplanetary magnetic field, *J. Geophys. Res.*, **98**, 187, 1993.

(Received July 14, 2000; accepted September 8, 2000)